



HAL
open science

VHF radar observation of atmospheric winds, associated shears and C_{2n} at a tropical location: interdependence and seasonal pattern

A. K. Ghosh, V. Siva Kumar, K. Kishore Kumar, A. R. Jain

► **To cite this version:**

A. K. Ghosh, V. Siva Kumar, K. Kishore Kumar, A. R. Jain. VHF radar observation of atmospheric winds, associated shears and C_{2n} at a tropical location: interdependence and seasonal pattern. *Annales Geophysicae*, 2001, 19 (8), pp.965-973. hal-00316888

HAL Id: hal-00316888

<https://hal.science/hal-00316888>

Submitted on 18 Jun 2008

HAL is a multi-disciplinary open access archive for the deposit and dissemination of scientific research documents, whether they are published or not. The documents may come from teaching and research institutions in France or abroad, or from public or private research centers.

L'archive ouverte pluridisciplinaire **HAL**, est destinée au dépôt et à la diffusion de documents scientifiques de niveau recherche, publiés ou non, émanant des établissements d'enseignement et de recherche français ou étrangers, des laboratoires publics ou privés.

VHF radar observation of atmospheric winds, associated shears and C_n^2 at a tropical location: interdependence and seasonal pattern

A. K. Ghosh, V. Siva Kumar, K. Kishore Kumar, and A. R. Jain

National MST Radar Facility, P. B. No.-123, Tirupati 517 502, India

Received: 5 September 2000 – Revised: 7 May 2001 – Accepted: 15 May 2001

Abstract. The turbulence refractivity structure constant (C_n^2) is an important parameter of the atmosphere. VHF radars have been used extensively for the measurements of C_n^2 . Presently, most of such observations are from mid and high latitudes and only very limited observations are available for equatorial and tropical latitudes. Indian MST radar is an excellent tool for making high-resolution measurements of atmospheric winds, associated shears and turbulence refractivity structure constant (C_n^2). This radar is located at Gadanki (13.45° N, 79.18° E), a tropical station in India. The objective of this paper is to bring out the height structure of C_n^2 for different seasons using the long series of data (September 1995 – August 1999) from Indian MST radar. An attempt is also made to understand such changes in the height structure of C_n^2 in relation to background atmospheric parameters such as horizontal winds and associated shears. The height structure of C_n^2 , during the summer monsoon and post-monsoon season, shows specific height features that are found to be related to Tropical Easterly Jet (TEJ) winds.

It is important to examine the nature of the radar back scatterers and also to understand the causative mechanism of such scatterers. Aspect sensitivity of the received radar echo is examined for this purpose. It is observed that radar back-scatterers at the upper tropospheric and lower stratospheric heights are more anisotropic, with horizontal correlation length of 10–20 m, as compared to those observed at lower and middle tropospheric heights.

Key words. Meteorology and atmospheric dynamics (climatology; tropical meteorology; turbulence)

1 Introduction

Study of the nature and characteristics of the atmospheric turbulence is of basic importance for understanding the atmospheric dynamics and coupling processes. It is well known that the intensity and nature of the atmospheric turbulence

depend on background atmospheric parameters such as atmospheric wind, temperature and humidity (VanZandt et al., 1981). These atmospheric parameters depend on the latitude of the station and the season. The atmospheric turbulence parameters are therefore expected to show large seasonal dependence (Nastrom et al., 1986). At tropical latitudes the turbulence parameters are expected to show distinct seasonal variations due to the presence of weather phenomena such as the South-West monsoon and the associated Tropical Easterly Jet (TEJ) winds.

MST radar is an excellent tool for making high-resolution measurements of atmospheric winds, associated vertical shears of horizontal winds and various atmospheric turbulence parameters. However, most of such studies are confined to mid and high latitudes (VanZandt et al., 1978; Smith et al., 1983; Nastrom et al., 1986) and only a few measurements are available at low latitudes (Sato and Woodman, 1982; Tsuda et al., 1985; Jain et al., 1995; Narayana Rao et al., 1997). The received radar echo intensity is generally used for determination of the parameter refractivity structure constant (C_n^2). The received radar echo intensity for the zenith beam is due to back-scatter from refractivity structure associated with atmospheric turbulence and also Fresnel reflection/scatter from gradients in the potential radio refractive index (M) (Röttger and Liu, 1978; Gage et al., 1978). At oblique angles, with beam zenith angle (χ) greater than or equal to 10° (i.e. $\chi \geq 10^\circ$), it is generally presumed that echos arise mainly due to radio refractivity structures associated with turbulence (Hooper and Thomas, 1998). The received radar echo intensity is therefore aspect sensitive and this particular feature is utilised to determine the horizontal correlation length and the characteristics of the radar back-scatterers giving rise to observed echo (Hooper and Thomas, 1995; Jain et al., 1997). In the present paper, Indian MST radar observations for four years, September 1995 – August 1999, are utilized to bring out the height structure of C_n^2 for different seasons. An effort is also made to understand the seasonal changes in C_n^2 in terms of background atmospheric parameters such as horizontal winds and associated vertical

Table 1. Values of radar parameters used in the computation of η and C_n^2

Symbols	Parameter	Values
λ	Radar Wavelength	5.66 m
Δr	Range Resolution	150 m
A_e	Effective antenna area	$1.2 \times 10^4 \text{ m}^2$
K_B	Boltzmann's Constant	$1.38 \times 10^{23} \text{ J/K}$
B_N	Receiver bandwidth (effective)	$1.7 \times 10^6 \text{ Hz}$
α_r	Receiver path loss	4.4 dB
α_t	Transmitter path loss	2.65 dB
T_C	Cosmic noise temperature	6000 K
T_r	Receiver noise temperature	607 K
N_B	Number of bauds for coded pulse	16
N_C	Number of coherent integration	128 (Table 1)
r	Range of back-scatter echo in metre	

shears. These observations have also brought out specific features of height structure of C_n^2 during the tropical monsoon season and the same are seen to be related to the easterly jet winds, near the tropopause, prevalent in the summer monsoon season.

2 Observations and method of computing C_n^2

Indian MST radar is a very sensitive, coherent, pulse Doppler radar with peak power aperture product of $3 \times 10^{10} \text{ Wm}^2$. The technical features of this radar are discussed by Jain et al. (1994) and Rao et al. (1995). The major parameters of the radar are given in Table 1. In the present study, daily evening common mode observations made using Indian MST radar during the period from September 1995 – August 1999 are utilised. Figure 1 shows the histogram of number of days of observations for each month during the period of observation. The measurements have been carried out every day for about 45 min during evening time between 16:30 to 17:15 (IST) (i.e. 11:00–11:45 UT). The experimental specification file (ESF) used for these experiments is given in Table 2. These measurements have height, time and velocity resolution of 150 m, 2 min and 0.2 m/s respectively and covered the height range of 3.6 to 32 km. For these measurements six beams, were used (see Table 2). The techniques used for signal and data processing are discussed by Anandan (1996). The zeroth moment of the spectrum received from the radar echo is used to compute the signal to noise ratio (\overline{SNR}). The mean SNR (i.e. SNR) for all the oblique beams, for each day, is used for the computation of the radar volume reflectivity (η) and C_n^2 . The expression used for computations of parameters η and C_n^2 are given as (Jaya Rao, 1998; Ghosh et al., 2000)

$$\eta = \frac{32(\log_e 2) K_B B_N (\alpha_r T_c + T_r) r^2}{P_t \alpha_r \alpha_t A_e N_B N_C \Delta r} \left(\frac{S}{N} \right)_o \quad (1)$$

where $(S/N)_o$ is SNR for oblique beams and P_t is the peak transmitted power; other symbols used in Eq. (1) are defined

Table 2. Experimental specification file (ESF) for the measurements using Indian MST radar

Parameter	Specifications
Pulse width (μs)	: 16
Inter pulse period (μs)	: 1000
Coded/Uncoded	: Coded (16 baud code, each baud=1?s)
Range resolution	: 150 m
No. of beams	: 6(E10y, W10y, Zy, Zx, N10x, S10x)*
Coherent Integration	: 128
No. of FFT points	: 128
Nyquist frequency (Hz)	: ± 4
Doppler resolution (Hz)	: 0.06
Observational window:	
Lowest range bin (km)	: 3.6
Highest range bin (km)	: 32
No. of incoh. integration	: 1
Beam dwell time	: ~ 16 sec
STC length (μs)	: 40
No. of scan cycle	: 8

* E 10y = Beam direction 10° east from the zenith in the East-West plane
W10y = Beam direction 10° west from the zenith in the East-West plane
Zy = Vertical beam direction formed using the East-West plane array
Zx = Vertical beam direction formed using the North-South plane array
N10x = Beam direction 10° north from the zenith in the North-South plane
S10x = Beam direction 10° south from the zenith in the North-South plane

in Table 1.

The turbulence refractivity structure constant C_n^2 is related to the radar volume refractivity

$$\eta = 0.38 C_n^2 \lambda^{-\frac{1}{3}} \quad (2)$$

After substituting the values of the various parameters given in Tables 1 and 2, Eqs. (1) and (2) can be rewritten as

$$\log_{10} \eta = -20.699 + \log_{10} r^2 - \log_{10} P_t + \frac{1}{10} \left(\frac{S}{N} \right)_{dB} \quad (3)$$

$$\log_{10} C_n^2 = -20.02 + \log_{10} r^2 - \log_{10} P_t + \frac{1}{10} \left(\frac{S}{N} \right)_{dB} \quad (4)$$

where $(S/N)_{dB}$ is the SNR for oblique beams in dB. In the present study, Eq. (4) is used for the determination of C_n^2 . It should, however, be mentioned here that the actual value of P_t for each day of observation is used for the computation of C_n^2 . The mean oblique and vertical beam \overline{SNR} is used to determine the echo aspect sensitivity and the horizontal correlation length of the radar backscatterers adapting the standard method (Hocking et al., 1989, 1990; Hooper and Thomas, 1995 and Jain et al., 1997). The horizontal correlation length

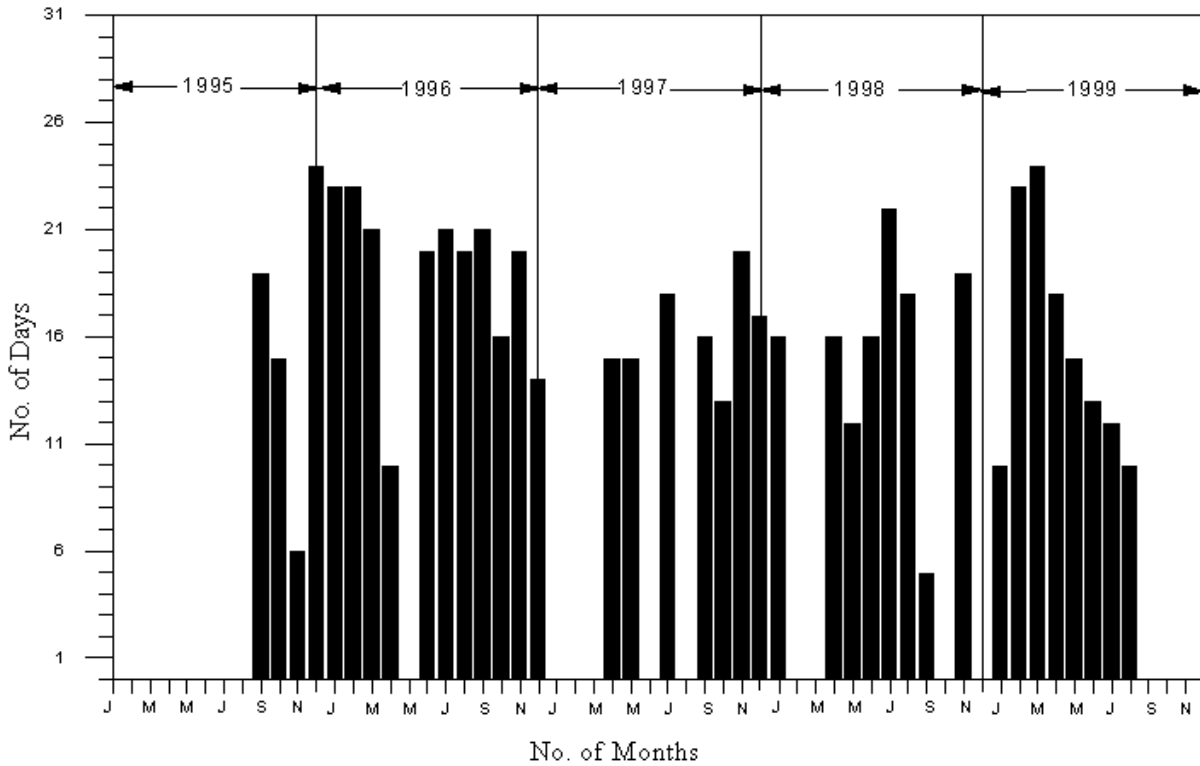


Fig. 1. Histogram showing the number of days of MST radar observations for each month during the period September 1995 to August 1999.

gives an idea of the horizontal length and anisotropy associated with the back-scatterers and is given by

$$\zeta = 15.2 \frac{\lambda}{\theta_s} \tag{5}$$

where λ is the radar wavelength and θ_s is e^{-1} of the half width the polar diagram of the radar backscatter expressed in degrees. Small values of θ_s means large anisotropic scattering. Received signal intensity (SNR) at the vertical and oblique beam is used for determination of θ_s (Hocking, 1986; Hocking et al., 1990; Hooper and Thomas, 1995).

3 Results

3.1 Monthly mean height profiles of horizontal winds (U_H), vertical shear of horizontal winds (s) and refractivity turbulence structure constant (C_n^2)

Figures 2, 3 and 4 represents, for each year, the monthly mean height profiles of U_H , s and C_n^2 . These figures show the height structure of the parameters for each month and so it is possible to examine month-to-month and also seasonal change of the parameters. South-West monsoon is a prominent weather phenomenon in the Tropical region of India. Therefore, the atmospheric changes can be understood with reference to monsoon conditions and the year is accordingly divided into four seasons viz., Winter (December, January and February), Pre-monsoon (March, April and May),

Monsoon (June, July and August) and Post-monsoon season (September, October and November).

3.1.1 Monsoon season

As seen from Fig. 2, Tropical Easterly Jet (TEJ) associated winds are observed in this season at the altitude range of 14–16 km. Here, range refers to the height intervals under discussion. Strong jet winds are observed during July and August. Strong vertical shears associated with strong jet winds are observed at the upper edge of TEJ in the height range of 16–18 km. An examination of the height profiles of C_n^2 shows a secondary peak between 16–19 km suggesting that enhanced radar reflectivity (η) and C_n^2 may be caused by enhanced wind shears present in these height ranges, which are upper edge of the TEJ (see Figs. 3 and 4).

3.1.2 Post monsoon season

As seen from Fig. 2, the easterly winds continue to prevail in September and October. However, during these months winds are weaker as compared to jet winds prevalent in monsoon months. In the month of November, however, these peak winds are absent. Accordingly, as seen from the Fig. 3, shears of magnitude $0.01\text{--}0.02 \text{ s}^{-1}$ are observable in the height range 16–19 km but in the month of November shears are relatively weak ($< 0.01 \text{ s}^{-1}$). The secondary peak in C_n^2 is observable in month of September and October also in the same height range but clearly much weaker for in November (see in Fig. 4). These results thus clearly indicate that

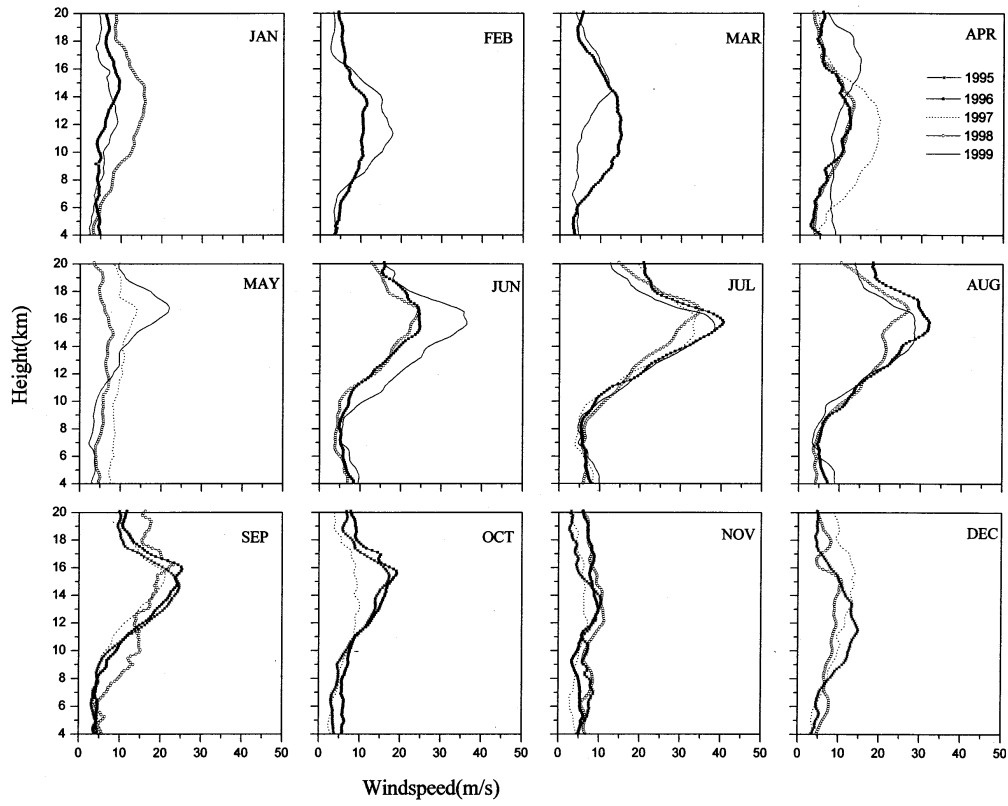


Fig. 2. Monthly mean height profiles of Wind speed for each month during the period September 1995 – August 1999.

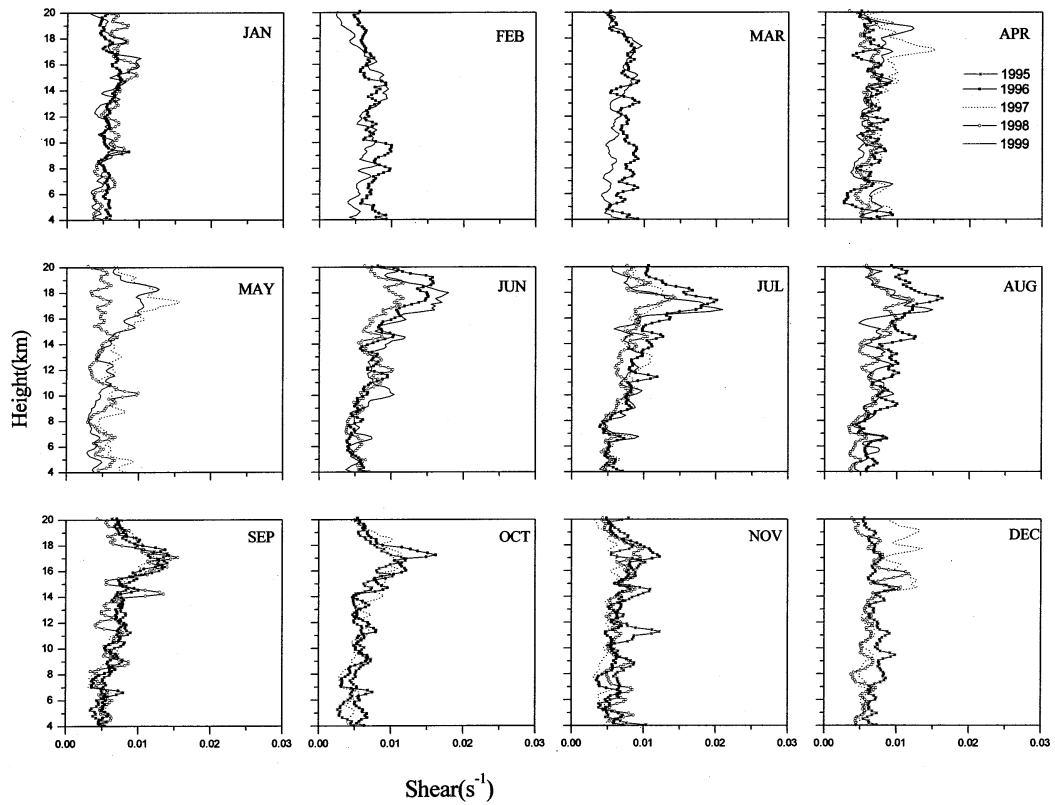


Fig. 3. Same as Fig. 2 but for vertical shear of horizontal wind.

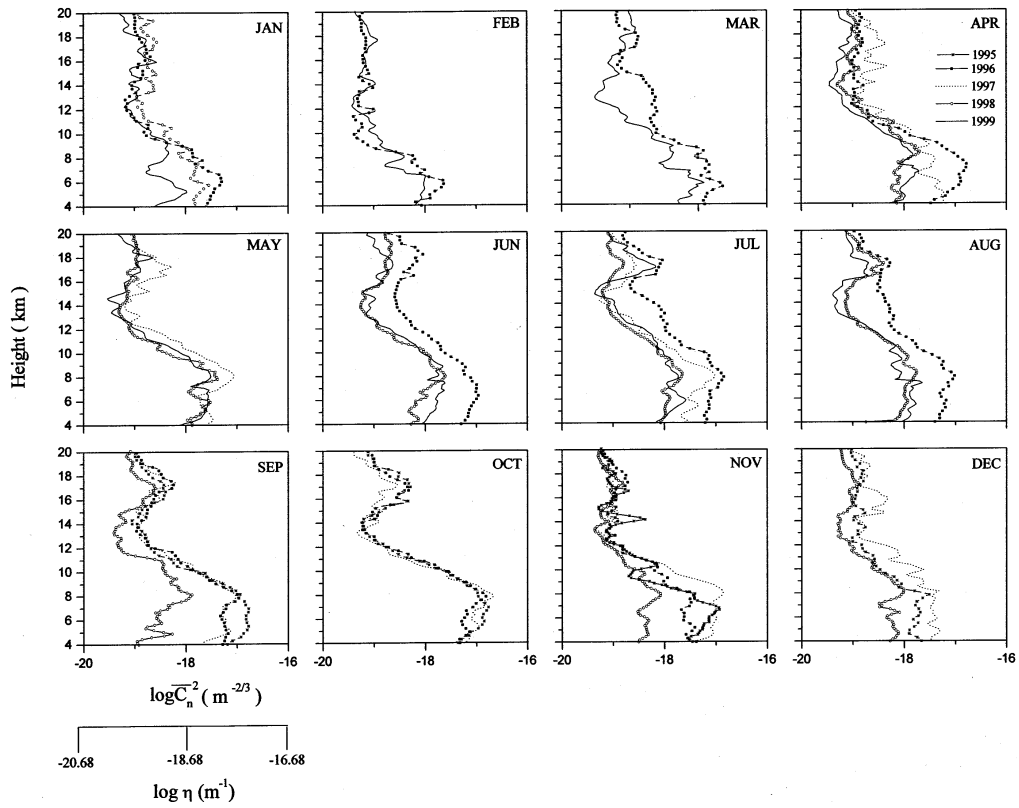


Fig. 4. Same as Fig. 2 but for turbulence refractivity structure constant $\log C_n^2$. The scale of radar reflectivity (η) is also marked in the figure.

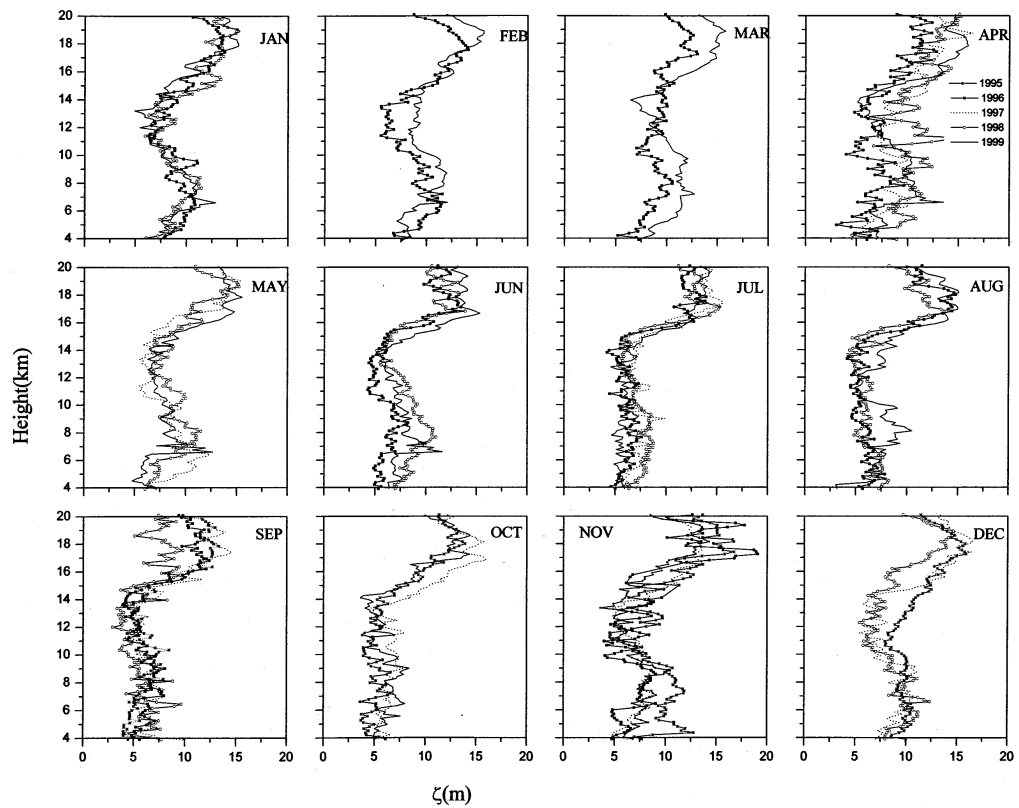


Fig. 5. Same as Fig. 2 but for horizontal correlation length ζ .

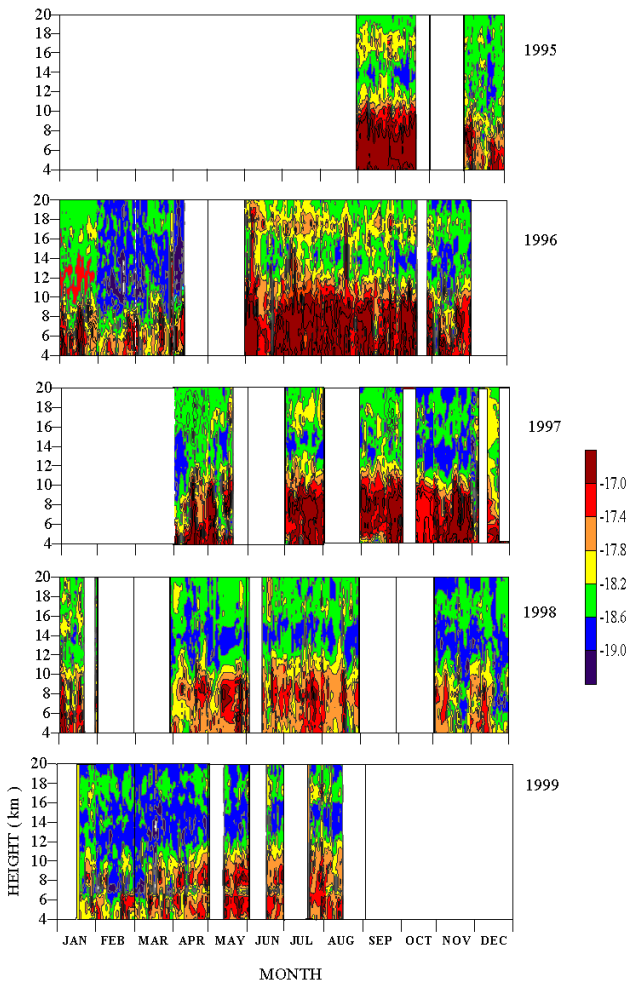


Fig. 6. HeightMonth and $\log C_n^2$ contour maps for the period September 1995 – August 1999. Vertical white bands represent the data gaps.

shears are contributing to enhanced radar reflectivity and C_n^2 . A distinct minimum is observable in C_n^2 in the height range of 12–16 km in monsoon and post monsoon months. This minimum could be due to lack of wind shears (see Fig. 3) or it may be due to weak potential refractive index gradient (M), in this height range.

3.1.3 Winter season

In these months, winds are relatively weak and peak winds (10–20 m/s) are in the height range of 10–14 km. Accordingly, shears are also very weak (see Fig. 3) and therefore there is no clear secondary peak is observable in η and C_n^2 in the height range of 14–19 km. The value of C_n^2 above 12 km is almost constant (see Fig. 4).

3.1.4 Pre-monsoon season

The winds continue to be very weak in the months of March and April as in the case of winter months and, accordingly, associated shears are also weak (see Figs. 2 and 3); there

is no clear secondary peak in η and C_n^2 in the height range 14–19 km. In month of May, however, the wind patterns are different and easterly winds in some years are observable with a peak between 16–19 km (see Fig. 2) and corresponding shears and secondary peak in η and C_n^2 is also seen (Figs. 3 and 4). Therefore, for these years the height structure of C_n^2 in May is similar to that observable in monsoon and post-monsoon months.

3.2 Monthly mean height profiles of horizontal correlation length (ζ)

The monthly mean height profiles of ζ are presented in Fig. 5. From these figure it is clear that values of ζ above 16 km are \sim 10–15 m which are much larger than the value of 5–10 m observed in lower and mid troposphere. This suggests that more anisotropic scatterers are present at the heights above 16 km. This is expected due to the temperature inversion associated with the tropopause and other stable layers present in lower stratosphere. This suggests that, above 16 km, enhanced static stability represented by N^2 could also contribute to the enhanced radar reflectivity. A recent paper by Jain et al., 2001, discussed these aspects in more details.

3.3 Contour maps of C_n^2

To get an over all idea of the month-to-month and year-to-year variability of height structure of C_n^2 , heightmonth contour maps of C_n^2 intensity are drawn for different years and these are presented in Fig. 6. The following points can be noted:

- The large year-to-year variability is noticeable in the height structure of C_n^2 for all the months.
- The band of minimum C_n^2 between 10–16 km is broader in height range during winter and pre-monsoon months as compared to remaining months.
- The secondary peak in C_n^2 is distinctly visible in monsoon and post-monsoon months between 16–19 km. However, in some years, for example in 1996, it is comparatively stronger than for other years. This again brings out year-to-year variability in C_n^2 .

3.4 Seasonal and month-to-month variation of C_n^2 height structure

Figure 7 shows the mean height profiles for each season for different years to bring out the variability of the height structure of C_n^2 . The following points can be seen in this figure:

- The secondary peak in C_n^2 , as discussed earlier, is clearly seen for monsoon and post-monsoon months. The values of C_n^2 at the height of about 17 km are close to the value of C_n^2 at the altitude of about 10 km.
- In winter months, the values of C_n^2 are minimal compared to other months and above 12 km values of C_n^2 are more or less constant.
- In pre-monsoon months, considerable year-to-year variability is observed in the height structure of C_n^2 . This is consistent with large variability of the observed winds and shears

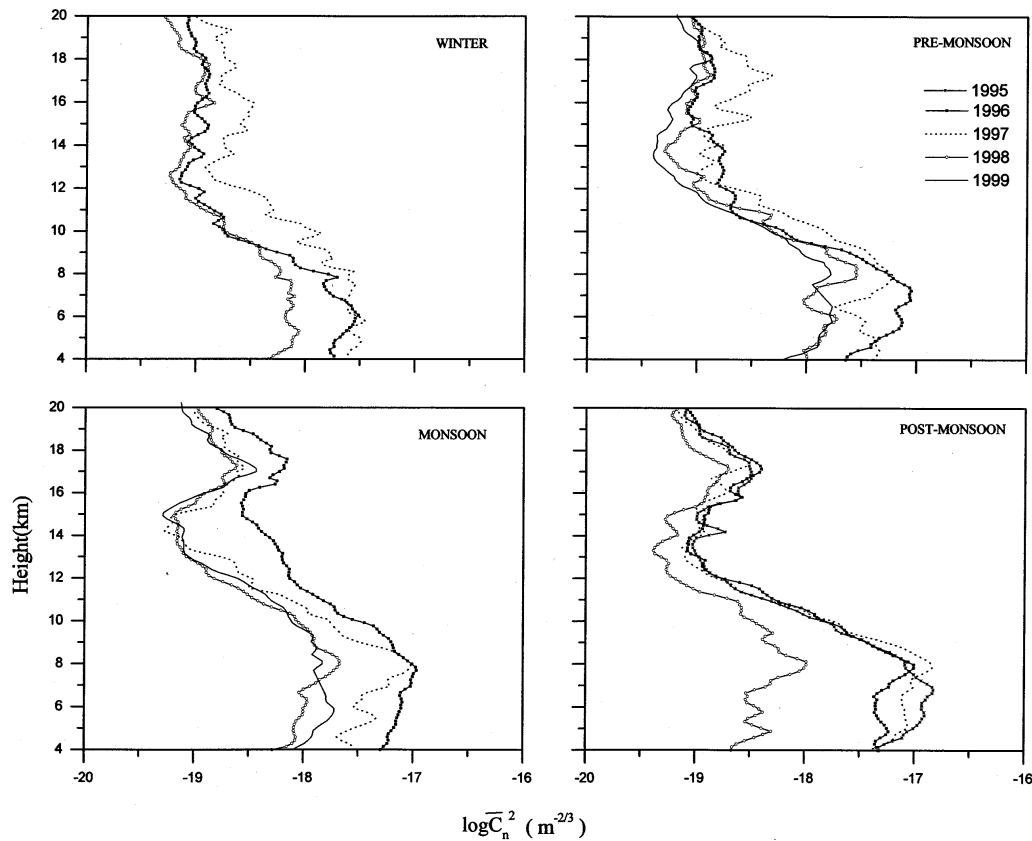


Fig. 7. Mean height profiles of $\log C_n^2$ for each season i.e. Winter, Pre-monsoon, Monsoon and Post-monsoon for each year of observation.

at this latitude during these months i.e. March, April and May (see Fig. 2).

In addition to the seasonal variation, month-to-month variation of C_n^2 is also examined, as shown in Fig. 8. In this figure panel [A] and [B] shows the plots of monthly mean C_n^2 obtained using all the available data for each month at nine heights. The following points emerged clearly from this figure:

i) The parameter C_n^2 is minimum in the month of February and March at all heights but this minimum is more distinct at heights above 15 km.

ii) The parameter C_n^2 shows an almost a flat peak for the months of May to October at lower heights and June to October at higher heights.

These results are consistent with those presented in Figs. 4, 6 and 7.

4 Discussion and conclusion

The turbulence refractivity structure constant (C_n^2) is one of the basic parameters of atmospheric turbulence which can be determined using the radar measurements of the received radar echo intensity (for example see VanZandt et al., 1978; Hocking et al., 1989). The radar echo arises due to refractive index irregularities, associated with turbulence on a scale equal to half of the radar wavelength $\lambda/2$). For Indian MST

radar, which operates at 53 MHz, half of the radar wavelength is about 3 m and thus, the radar samples the refractive index irregularities of this scale.

Most of the observation of C_n^2 using VHF radars have been carried out at mid and high latitudes (VanZandt et al., 1978; Gage et al., 1978, 1980; Hocking et al., 1989; Smith et al., 1983; Nastrom et al., 1986); only a few measurements are available at tropical and low latitude regions (Sato and Woodman, 1982; Tsuda et al., 1985; Narayana Rao et al., 1997). Therefore, more measurements are necessary to have a better idea of C_n^2 in this region. Jain et al. (1995) presented first measurements of C_n^2 in the height range of 4–11 km using Indian MST radar in ST mode with a peak power aperture product of $4.8 \times 10^6 \text{ Wm}^2$. Narayana Rao et al. (1997) have presented measurements of C_n^2 made using Indian MST radar in MST mode with an average power aperture product of $3 \times 10^{10} \text{ Wm}^2$. These authors made use of one year of observations taken during the period January 1993 to December 1993. In the present paper, four years of evening common mode observations for the period September 1995 to August 1999 are utilized for the determination of C_n^2 . These measurements are analyzed to examine the height structure of C_n^2 at this tropical station in India. An effort is also made to bring out the seasonal features of the C_n^2 height structure and relate the same to the background atmospheric winds and vertical shears associated with these winds.

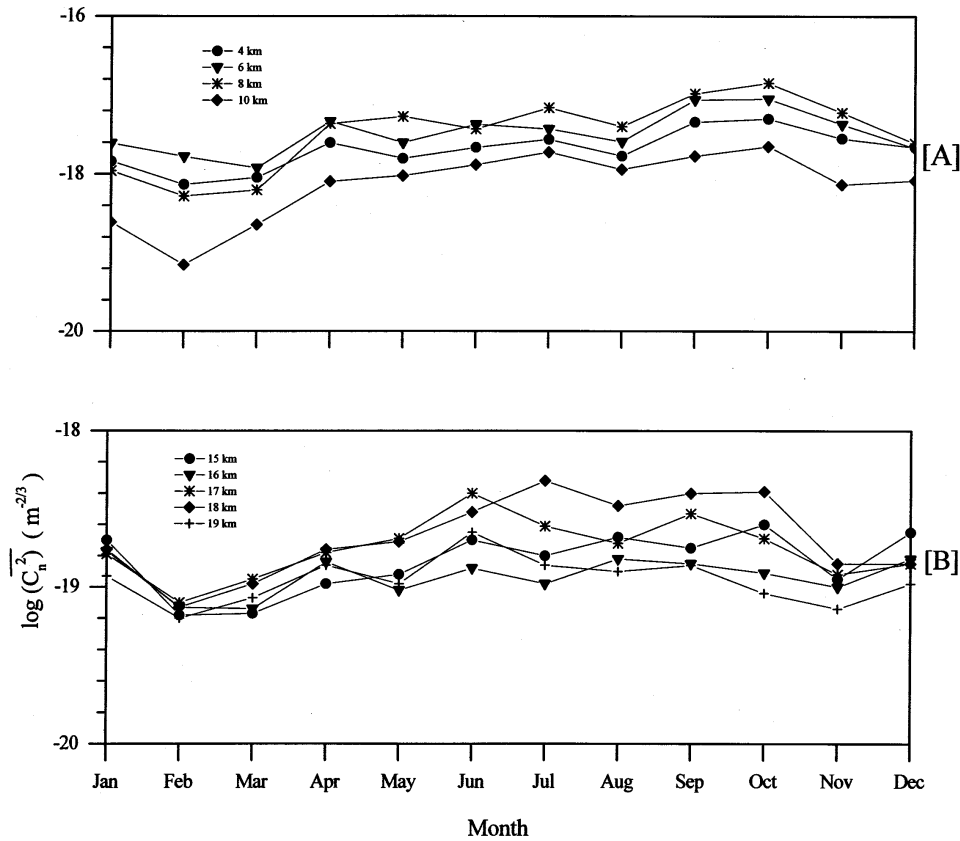


Fig. 8. Plots of monthly mean C_n^2 , taken over the four years of observations, at nine different heights in the troposphere and the lower stratosphere, [A] 4–10 km and [B] 15–19 km.

Some interesting results are brought out from this study. In monsoon and post-monsoon seasons, a secondary peak is observed in C_n^2 in the height range of 16–20 km and a minimum in the height range of 12–16 km. This secondary peak in C_n^2 is found to be closely associated with the vertical shear of horizontal winds that are observed to occur at the upper edge of the TEJ. In winter and the pre-monsoon season, the secondary peak in C_n^2 is absent and almost constant values of C_n^2 are observed for heights above 12 km. This height structure of C_n^2 is noted to be consistent with weak horizontal winds and associated shears observed in these seasons. The height structures of C_n^2 in winter and the pre-monsoon season are significantly different than those observed in monsoon and post-monsoon season. From these results it is evident that the presence of strong wind shears does contribute to the height structure of C_n^2 significantly. Tsuda et al. (1985), using high-resolution measurements with the Aerico radar, show that there is a good correlation between echo power and wind shear. Several measurements of atmospheric turbulence associated with jet stream due to strong shears show enhancement in C_n^2 (Gage et al., 1980; VanZandt et al., 1981; Smith et al., 1983). However, most of these results are confined to mid latitudes.

The month-to-month variation of C_n^2 is also examined in details. The parameter C_n^2 is found to show a clear mini-

mum at all heights in the months of February and March and may be due to the lack of wind shear and humidity. The value of C_n^2 is almost constant during May–October months at lower heights i.e. 4–10 km, and for the months of June–October at greater heights. High humidity during the months of May–October at a lower height is the most likely cause of enhanced C_n^2 during these months. At greater heights, enhanced wind shears, observed during June–October, appear to contribute significantly to enhanced C_n^2 during this period. Narayana Rao et al. (1997) have also reported a similar monthly variation of C_n^2 for Gadanki. However, in the present study an attempt is also made to relate the same to the background atmospheric parameters for a better understanding of the causative mechanism of turbulence. In addition to the significant month-to-month and season-to-season variability in height structure of C_n^2 , considerable year-to-year variability is also observed. These variabilities need to be taken into account in designing new atmospheric radar for studies at tropical latitudes.

Acknowledgement. The National MST Radar Facility (NMRF) is set up jointly by the Council of Scientific and Industrial Research (CSIR), Defence Research and Development Organization (DRDO), Department of Electronics, Environment, Science and Technology and Space, Govt. of India with the Department of Space as a nodal agency. The NMRF is operated by the Department of Space, Govt. of India, with partial support from CSIR. We wish to

thank the staff of the National MST Radar Facility for their support in collection of data used in this paper. We thank the anonymous reviewers, whose suggestions have resulted in substantial improvement of the paper.

Topical Editor J.-P. Duvel thanks R. Schumann and another referee for their help in evaluating this paper.

References

- Anandan, V. K., Balamuralidhar, P., Rao P. B., and Jain, A. R., A method for adaptive moments estimation technique applied to MST radar echoes, Progress in electromagnetic research symposium, Telecommunication research center, City university of Hongkong, 1996.
- Gage, K. S., VanZandt T. E., and Green, J. L., Vertical profiles of C_n^2 in the free atmosphere: Comparison of model calculations with radar observations, 18th conference on Radar Meteorology, Pre vol., 80–87, A. M. S., Boston, MAS, 1978.
- Gage, K. S., Green, J. L., and VanZandt, T. E., Use of Doppler radar for the measurements of atmospheric turbulence parameters from the intensity of clear air echoes, Radio Sci., 15, 407–417, 1980.
- Ghosh, A. K., Jain, A. R., and Siva Kumar, V., Characteristics of atmospheric wind, associated shear and turbulence: Indian MST radar measurement during summer monsoon season, Indian J. Radio and Space Phys., 29, 222–230, 2000.
- Hocking, W. K., Observations and measurements of turbulence in the middle atmosphere with VHF radar, J. Atmos. Terr. Phys., 48, 655–670, 1986.
- Hocking, W. K., Lawry K., and Neudegg, D., Radar measurements of atmospheric turbulence intensities by C_n^2 and spectral width method, Middle Atmospheric program Hand Book, 27, 443–446, SCOSTEP Secretariat, Univ. Illinois, 1989.
- Hocking, W. K., Fukao, S., Tsuda, T., Yamamoto, M., and Kato, S., Aspect sensitivity of stratospheric VHF radio wave scatterers particularly above 15 km altitude, Radio Sci., 25, 613–627, 1990.
- Hooper, D. A. and Thomas, L., Aspect sensitivity of VHF scatterers in the troposphere and stratosphere from comparisons of power in off-vertical beams, J. Atmos. Terr. Phys., 57, 655–663, 1995.
- Hooper, D. A. and Thomas, L., Complementary criteria for identifying regions of intense atmospheric turbulence using lower VHF radar, J. Atmos. Solar Terr. Phys., 60, 49–61, 1998.
- Jain, A. R., Jaya Rao, Y., Rao, P. B., Viswanathan, G., Damle, S. H., Balamuralidhar, P., and Kulkarni, A., Preliminary observations using ST mode of the Indian MST radar. Detecting the signature of the tropopause, J. Atmos. Terr. Phys., 56, 1157–1162, 1994.
- Jain, A. R., Jaya Rao, Y., Rao, P. B., Anandan, V. K., Damle, S. H., Balamuralidhar, P., Kulakerni, A., and Viswanathan, G., Indian MST radar, 2. First scientific results in ST mode Radio sci., 30, 1139–1158, 1995.
- Jain, A. R., Jaya Rao, Y., and Rao, P. B., Aspect sensitivity of the received radar back scatter at VHF: Preliminary observations using Indian MST radar, Radio Sci., 37, 1249–1260, 1997.
- Jain, A. R., Jaya Rao, Y., and Mydhili, N. S., Height-time-structure of VHF backscatter from stable and turbulently mixed atmosphere layers at tropical latitudes, J. Atmos. Solar Terr. Phys., in press, 2001.
- Jaya Rao, Y., A study of atmospheric stable layers in the Tropical Atmosphere using Indian MST Radar., Ph. D. Thesis, Sri Venkateshwara University, Tirupati, 1998.
- Narayan Rao, D., Kishore, P., Narayan Rao, T., Vijaya Bhaskara Rao, S., Krishna Reddy, K., Yarraiah, M., and Hareesh, M., Studies on refractivity structure constant, eddy dissipation rate and momentum flux at a tropical latitude, Radio Sci., 32, 1375–1389, 1997.
- Natrom, G. D., Gage, K. S., and Ecklund, W. L., Variability of turbulence, 4–20 km, in Colorado and Alaska from MST radar observations, J. Geophys. Res., 91, 6722–734, 1986.
- Rao, P. B., Jain, A. R., Kishore, P., Balamuralidhar, P., Damle, S. H., and Viswanathan, G., Indian MST radar, 1, System description and sample vector wind measurements in ST mode, Radio Sci., 30, 1125–1138, 1995.
- Röttger, J. and Liu, C. H., Partial reflection and scattering of VHF radar signals from clear atmosphere, Geophys. Res. Lett., 5, 357–360, 1978.
- Sato, T. and Woodman, R. F., Fine altitude resolution observations of stratospheric turbulent layers by the Arecibo 430-MHz radar, J. Atmos. Sci., 39, 2546–2552, 1982.
- Smith, S. A., Romick, G. J., and Jayaweera, K., Poker Flat MST observations of shear-induced turbulence, J. Geophys. Res., 88, 5265–5271, 1983.
- Tsuda, T., Hirose, K., Kato, S., and Sulzer, M. P., Some finding on correlation between the stratospheric echo power and the wind shear observed by the Arecibo UHF radar, Radio Sci., 20, 1503–1508, 1985.
- VanZandt, T. E., Green, J. L., Gage K. S., and Clark, W. L., Vertical profiles of refractivity turbulence structure constant: Comparison of observations by the sunset radar with a new theoretical model, Radio Sci., 13, 819–829, 1978.
- VanZandt, T. E., Gage, K. S., and Warnock, J. M., An improved model for the calculation of profiles of C_n^2 and ϵ in the free atmosphere from background profiles of wind, temperature and humidity, in proceedings of the 20th Conference on Radar Meteorology, pp 1290135, Am. Meteorol. Soc., Boston, Mass., 1981.